JOURNAL OF MATERIALS SCIENCE 33 (1998) 4159–4165

Growth of porous anodic films on FVS0812 aluminium alloy

J. A. SYKES, G. E. THOMPSON, P. SKELDON
Corrosion and Protection Centre, University of Manchester Institute of Science and Technology, PO Box 88, Manchester M60 1QD, UK
E-mail: p.skeldon@umist.ac.uk

D. MAYO
British Aerospace Defence Limited, Warton, Preston PR4 1AX, UK

The formation of porous anodic films on FVS0812 aluminium alloy has been examined by transmission electron microscopy in order to elucidate the processes of film growth. A complex morphology of film material is revealed containing relatively tortuous, branched and terminated porosity and relatively large cavities. The morphology is associated with the differing anodic oxidation behaviour of the aluminium matrix and silicide dispersion regions of the alloy and the differing chemical stabilities of the resultant film regions. The anodic oxidation of the silicide proceeds more slowly than that of the aluminium matrix, with the production of film material of much finer morphology. The reduced rate of oxidation of the silicide is attributed to the effects of alloying element species in the anodic film material and pore solution. The rate of oxidation of the silicide is sufficient for most of the particles to be oxidized completely during anodizing. However, the resultant film material subsequently dissolves in the pore solution leaving relatively large cavities in the film. The differing oxidation rates of the alloy components, coupled with locally differing film properties, leads to a relatively rough alloy/film interface.

1. Introduction

FVS0812 is a high-strength aluminium alloy, produced by rapid solidification technology, which, after consolidation, retains useful strength to 673 K [1]. The high temperature mechanical properties are associated with the presence of about 27 vol % of finely dispersed silicide phase, namely $Al_{13}(Fe, V)_3Si$, which resists coarsening at elevated temperature [2]. For certain aerospace applications, the alloy may need a protective coating. Thus, there is interest in the formation of porous anodic films on the alloy surface. However, previous studies suggest that porous film development is impaired on the alloy largely by the reactivity of the second phase material in the anodizing electrolyte [3, 4]. Consequently, a highly flawed film of relatively low thickness is produced.

In general, there has been relative confusion about the precise behaviour of second phase materials during anodizing of aluminium alloys, in particular $FeAl_3$ which, apart mainly from the absence of silicon, is similar in composition to the silicide phase of FVS0812 alloy. For instance, studies have concluded oppositely either that $FeAl_3$ particles are incorporated into the anodic film relatively unchanged [5], or that the particles are first oxidized [6]. Conclusive evidence of the oxidation of the particles has since been obtained recently from observations of ultramicrotomed sections of anodized alloy in the transmission electron microscope [7]. A similar approach to that of the last study has been applied to the FVS0812 alloy, although whether silicide particles are oxidized to form anodic film material was not fully resolved [4]. In view of the remaining uncertainty about the oxidation of silicide particles and the subsequent effects on general film development, the growth mechanism of porous anodic films on FVS0812 alloy is considered further here.

2. Experimental procedure

2.1. Specimen preparation

Specimens of FVS0812 alloy (4.3 at % Fe, 1.7 at % Si, 0.7 at % V, 8.5 % Fe, 1.7 % Si, 1.3 % V by weight), of dimensions $50 \times 10 \times 1.5$ mm, were mechanically polished to a 0.25 μm diamond finish. After thorough rinsing, the specimens were anodized at 100 A m^{-2} in stirred 1 M sulphuric acid at 298 K for times to 1800 s. The voltage–time response was recorded during anodizing of individual specimens. After anodizing, specimens were rinsed in deionized water and dried in a cool air stream. For purposes of comparison, films were formed on mechanically polished, high purity aluminium (99.99 %).

2.2. Specimen examination

Sections, ~10 nm thick, of the anodized alloy were prepared by ultramicrotomy for examination in a Jeol

FX 2000 II transmission electron microscope equipped with energy dispersive X-ray (EDX) analysis facilities. The compositions of films were investigated by Rutherford backscattering spectroscopy (RBS) using a 2.0 MeV beam of alpha particles supplied by the Van de Graaff accelerator of the University of Paris. The beam current and diameter were ~ 60 nA and ~ 1 mm, respectively. Particles were detected at 165° to the incident beam direction. Data were analysed by the RUMP program [8], with scaling of the stopping power for oxygen by 0.88 [9].

3. Results

3.1. Voltage–time response

The voltage–time response revealed an initial linear voltage rise to ~ 5 V, following which the slope gradually decreased until a maximum voltage of ~ 25 V was achieved after 300 s of anodizing (Fig. 1). With further anodizing, the voltage remained approximately constant to the maximum time of anodizing that was employed. Oxygen was evolved at the specimen surface shortly after the commencement of anodizing and persisted until the current was switched off. The voltage–time response for high purity aluminium was of the same general form as that for the FVS0812 alloy. However, a steady state voltage of ~ 14.6 V was achieved at 60 s of anodizing.

3.2. Transmission electron microscopy

The transmission electron micrograph of a specimen anodized for 1800 s reveals a 4.5 μm thick porous film of complex morphology attached to the alloy substrate (Fig. 2). The silicide particles are evident in the latter as darker regions in the aluminium matrix, of abundance corresponding closely to their expected volume fraction. The composition of the particles, determined by EDX, was consistent with the expected $Al_{13}(FeV)_3Si$ [1]. From examination of sections of the alloy, the average size of the silicide particles is ~ 56 nm. The sizes of some particles in the ultramicrotomed section appear smaller than their actual sizes since the section thickness, of about 10 nm, is much less than the average particle size. The particles are distributed non-uniformly within the aluminium matrix, with clusters of particles occurring in some locations.

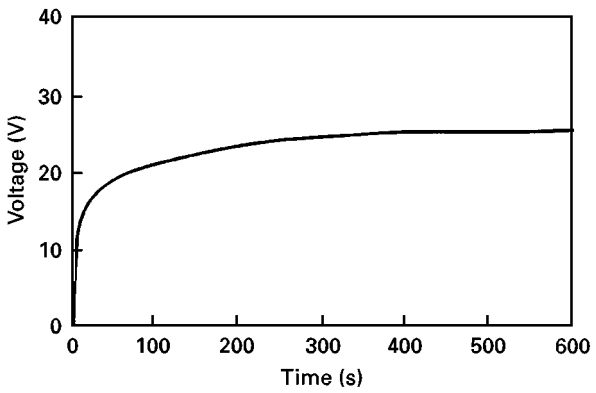

Figure 1 The typical voltage–time response for anodizing FVS0812 alloy at 100 A m^{-2} in 1 M sulphuric acid at 298 K.

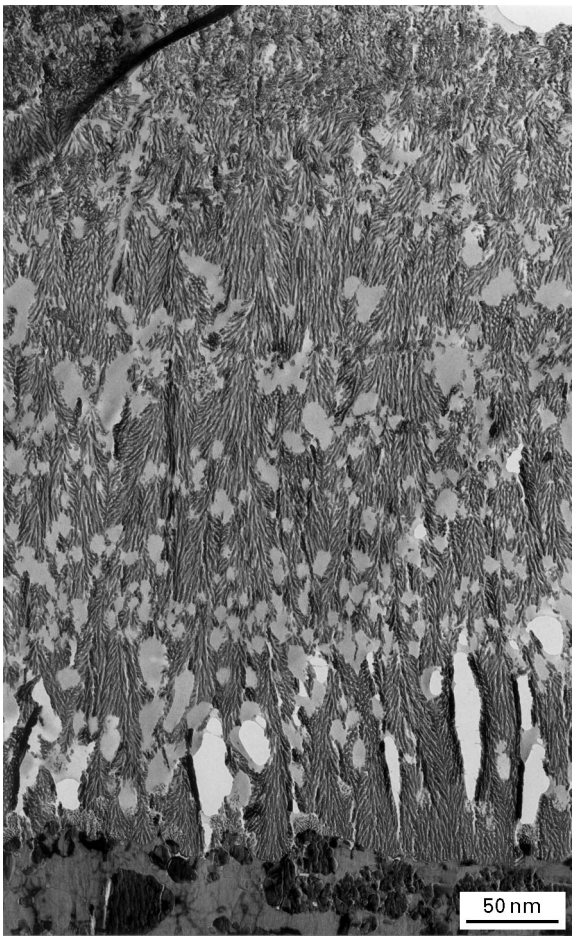

Figure 2 Transmission electron micrograph of an ultramicrotomed section of FVS0812 alloy anodized at 100 A m^{-2} in 1 M sulphuric acid at 298 K for 1800 s, showing the main film thickness.

The anodic film contains several major cracks near to the alloy/film interface; the cracks contain no resin, from mounting of the specimen for ultramicrotomy, indicating that they were produced during sectioning of the film. Fine, tunnel-like pores, that intermittently branch or terminate, are present throughout the main film. From examination of several sections, the complex pattern of pores suggests a typical pore diameter of ~ 11 nm for the main film material with an 8–10 nm thick barrier layer above regions of matrix material. The porosity is much less regular than that of a porous film grown under similar conditions on high purity aluminium, which contains approximately parallel pores, of 19 nm diameter near the pore base, normal to the alloy/film interface, with a barrier layer of 13 nm thickness (Fig. 3). The thickness of the film formed for 1800 s on high purity aluminium, namely 9.5 μm, is 2.1 times that formed on the FVS0812 alloy. In the film on the FVS0812 alloy, the pores in places are orientated at a wide range of angles with respect to the alloy/film interface. A further major distinguishing feature of the film is extensive larger porosity throughout most of the film thickness, with pore shapes and size similar to those of the second phase particles of the alloy. These larger pores are filled with resin, which confirms their presence in the film prior to ultramicrotomy.

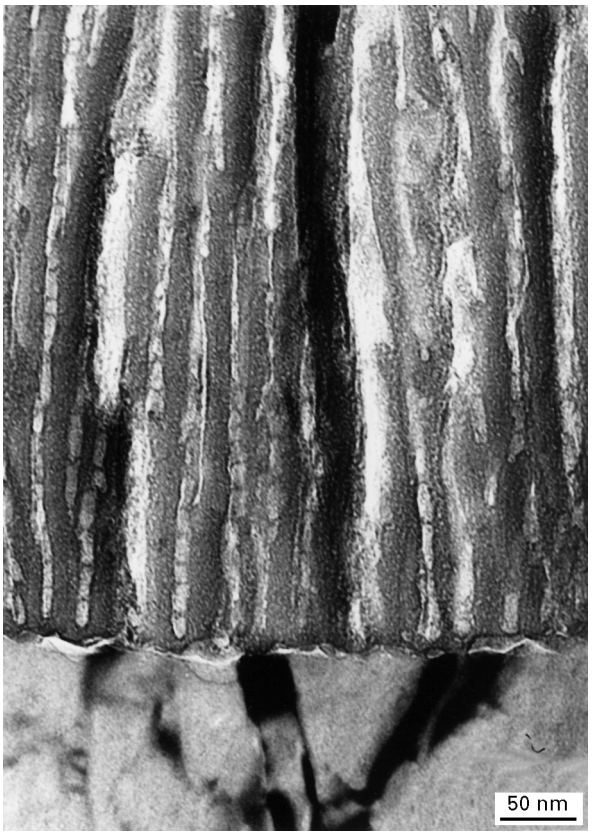

Figure 3 Transmission electron micrograph of an ultramicrotomed section of high purity aluminium anodized at 100 A m^{-2} in 1 M sulphuric acid at 298 K for 1800 s, showing the film morphology in the region of the metal/film interface.

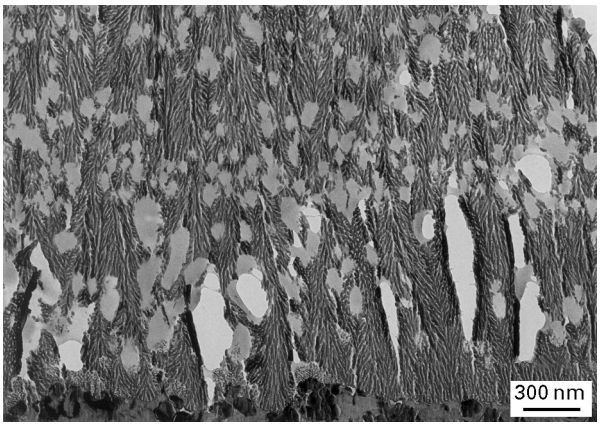

Figure 4 Transmission electron micrograph of an ultramicrotomed section of FVS0812 alloy anodized at 100 A m^{-2} in 1 M sulphuric acid at 298 K for 1800 s, showing the inner part of the film thickness and the region of the alloy/film interface.

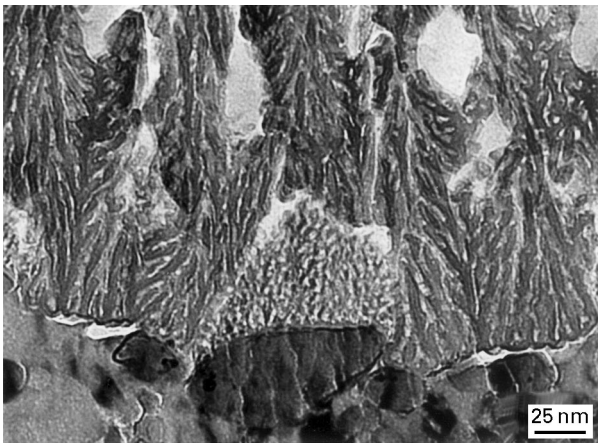

Figure 5 Transmission electron micrograph of an ultramicrotomed section of FVS0812 alloy anodized at 100 A m^{-2} in 1 M sulphuric acid at 298 K for 1800 s, showing a region of the alloy/film interface in more detail with a partially oxidized silicide particle.

More interesting detail of the film morphology is disclosed by higher magnification examination of the region near to the alloy/film interface (Fig. 4). The resin-filled, larger porosity of the main film material is absent from the innermost 150 nm of the film thickness. This innermost region comprises two distinct morphologies of porous film material, which are most easily discerned by comparing the porous material, adjacent to the alloy/film interface, developed above the aluminium matrix and silicide dispersion regions. Above the former, the morphology is indistinguishable from that of the main film which contains the relatively large porosity. In contrast, a finer morphology is developed above the silicide dispersoids. However, this finer material is absent from the main film.

Closer examination in the neighbourhood of the alloy/film interface shows clearly the fine, tortuous porosity of the film material that was growing upon a partially oxidized dispersoid, with the composition confirmed as silicide by EDX, at the termination of anodizing (Fig. 5). The geometry of the pores is not easily discerned from the film section, which is thicker than the scale of the porosity. Immediately above the region of finer film morphology formed on the partially oxidized, relatively large silicide, resin-filled cavities indicate locations originally containing similar fine material from the complete oxidation of finer silicide particles. The original film material has clearly dissolved following the oxidation of the silicide particles leaving cavities in the anodic film. Small, resin-filled cavities at the upper interface between the finer material formed upon the partially oxidized silicide and the material of the main film suggest that dissolution of the finer film has commenced prior to complete oxidation of the particular silicide. The barrier layer is $\sim$3 nm thick above regions of silicide, which is about one-third of that above matrix regions. The alloy/film interface, which moves inwards during anodizing of the alloy, has just reached other silicide particles adjacent to the partially oxidized silicide particle. These adjacent particles have not been anodically oxidized in the regions of the particles sampled by the ultramicrotomed section, which is evident from the relatively coarse morphology of the overlying oxide that characterizes the anodized matrix material. In places along the alloy/film interface, the anodic film is detached from the alloy substrate. The detachment may be caused by damage, during sectioning, of an interface which is either weakened by film stresses or contains pre-existing defects from the growth of the film.

There appear to be no cavities in the film material that are created by production of oxygen at high

pressure within the film. However, unlike barrier films which are sufficiently thick to retain oxygen in moderately large bubbles, to a few tens of nanometres in size [10], the thin barrier layer of the present porous films may readily release the oxygen due to a combination of mechanical rupture and rapid encroachment of the retreating barrier layer/electrolyte interface.

The alloy/film interface is relatively irregular with variations of ± 25 nm about the mean depth of the interface from the film surface. Observation of a longer length of the alloy/film interface reveals a tendency for high and low points of the interface to coincide with the regions of oxidizing dispersoid and aluminium matrix respectively (Fig. 6). At certain locations, partially oxidized dispersoid particles project significantly into the anodic film due to the greater depth of oxidation of the surrounding aluminium matrix. The pores in the material formed immediately above the aluminium matrix are orientated approximately normal to the local alloy/film interface. However, the local alloy/film interface can be orientated at a wide range of angles with respect to the mean interface location, thus giving rise to the varied orientation of pores in the main film.

3.3. RBS and EDX analyses

RBS analyses were carried on films formed for 60, 300 and 600 s in order to determine the amount of iron and vanadium species in the anodic films. Because of the similarity of the atomic masses of iron and vanadium the separate species were not distinguished. The presence of silicon species could not be determined because of the proximity of their atomic mass to that of aluminium. Typical experimental and simulated spectra reveal the presence of iron, vanadium and sulphur species in the anodic film (Fig. 7). For the thicker films, formed for 300 and 600 s, only the outer ~ 500 nm could be reliably analysed. The analyses revealed a progressive decrease in the average concentrations of iron and vanadium species with time of anodizing: the atomic ratios of (Fe + V)/Al were 0.045, 0.021 and 0.012, to $\sim 5\%$ accuracy, for anodizing times of 60, 300 and 600 s, respectively. The atomic ratio of S/Al in the film, ~ 0.1, was approximately the same at each anodizing time. The sulphur species incorporated into the anodic film at the barrier layer/electrolyte interface are derived from the anions of the sulphuric acid electrolyte.

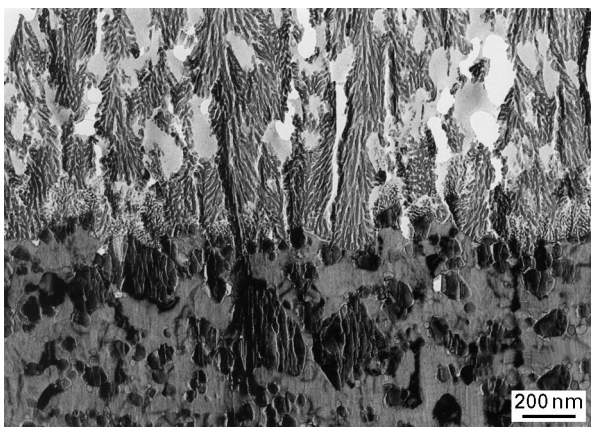

Figure 6 Transmission electron micrograph of an ultramicrotomed section of FVS0812 alloy anodized at 100 A m^{-2} in 1 M sulphuric acid at 298 K for 1800 s, showing the roughness of the alloy/film interface and silicide particles projecting into the film.

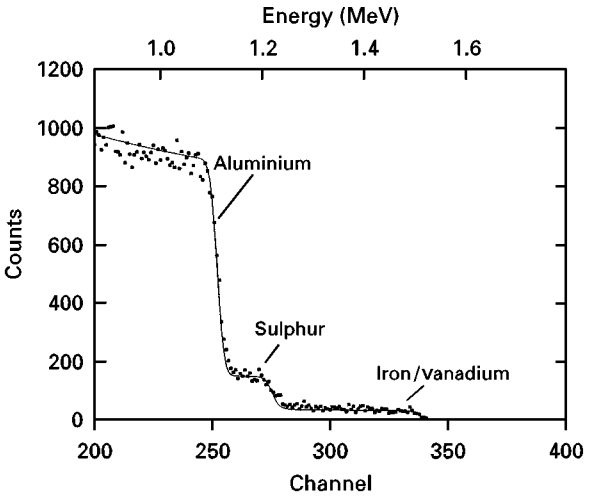

Figure 7 Experimental and simulated RBS spectra for FVS0812 alloy oxidized at 100 A m^{-2} in 1 M sulphuric acid at 298 K for 60 s showing the regions corresponding to scattering from alloying element species in the anodic film.

Several EDX analyses, using an electron beam of 75 nm diameter, of film material adjacent to the alloy/film and film/electrolyte interfaces, produced during 900 s of anodizing, revealed average atomic ratios of Fe/Al of 0.04 and 0.01, respectively. The latter value is consistent with the previous RBS analyses. The V/Al ratio also decreased between the two interfaces, from ~ 0.01 near the alloy/film interface to negligible levels near the film/electrolyte interface. The Si/Al ratio, ~ 0.04, was similar for the film material in the region of both interfaces.

4. Discussion

4.1. Porous film morphology

Transmission electron microscopy has revealed clearly the formation of porous anodic film material above both aluminium matrix and silicide dispersoid regions of FVS0812 alloy during anodizing in sulphuric acid electrolyte. The film morphology is more complex than that developed on high purity aluminium, due mainly to the influence of the dispersoid, which is consistent with the findings of previous work employing transmission electron microscopy [3, 4]. These other studies, including the use of *i–t* responses during potentiostatic polarization, cyclic voltammetry and a.c. impedance, found a greater reactivity of the dispersoid material, which was associated with the more complex film structure on the alloy. However, the experiments did not disclose the precise mechanism of anodic oxidation of the dispersoid material, and in particular whether or not porous oxide is formed above the dispersoid material during anodizing of the alloy and the nature of any resultant oxide

material. Importantly, the present work shows clearly that the dispersoid material is oxidized at the alloy/film interface, forming finely porous, oxide film material above a thin barrier layer. Further, the rate of oxidation of the dispersoid material is less than that of the adjacent material, but sufficiently fast for the shapes and sizes of the majority of dispersoid particles to result in complete oxidation of the particles as the alloy/film interface recedes during anodizing. This oxide material subsequently dissolves chemically in the anodizing electrolyte, leaving relatively large voids in the film. It is possible that occasional particles are not completely oxidized, because of their particular shape, size and location in the alloy. These findings are contrary to the previously suggested partial electro chemical dissolution of the dispersoid at the alloy/film interface followed by later chemical dissolution of incorporated residual dispersoid material [4]. Further, although a more distorted oxide morphology, compared with that formed on simulated matrix material, has been reported by others [4], the finer oxide morphology formed by anodic oxidation of the dispersoid regions was not revealed.

The finely porous film material grows more slowly on the dispersoid phase, evidenced by the tendency of partially oxidized dispersoid particles to project into the anodic film. This assists roughening of the alloy/film interface, leading to a wide range of orientations of pores in the general film material, and branching of pores during anodic oxidation of the alloy. The morphology of the porous film material formed on the matrix regions is close to that formed on high purity aluminium, in terms of thickness of the barrier layer and pore diameter, although the porosity is finer and less regular, because of the range of orientation, branching and termination of pores.

The film material associated with oxidized silicide is relatively unstable in the electrolyte and dissolves, subsequent to its formation, in the pore solution that permeates the porous film. Thus, the film contains relatively extensive additional porosity from dissolution of regions of oxidized silicide particles. The oxidized particles dissolve in about 60 s following their formation, which is the time required for the alloy/film interface to retreat a distance corresponding to the thickness of the layer of undissolved silicide film material, namely $\sim$150 nm. In contrast, chemical dissolution of the film material formed above aluminium matrix regions is comparatively negligible.

4.2. Mechanism of porous film growth

The complex film morphology on the FVS0812 alloy is linked intimately with the modified anodic oxidation of the silicide dispersoid, which contains $\sim$18 at % (Fe + V) and $\sim$6 at % Si [1], compared with that of the relatively pure aluminium matrix. The material constituting the main porous layer is formed initially at the alloy/film interface, with incorporation of aluminium and alloying element species into the barrier layer. Hence, consideration of the formation of barrier films is of relevance to the understanding of porous film growth. Barrier anodic film formation on the silicide phase results in alumina film material contaminated by alloying element species [10]. The concentration of iron, and probably vanadium, species in the main film is reduced compared with that in the dispersoid phase due to faster migration of iron and vanadium species than that of Al^{3+} ions [10]. The behaviour of silicon species is less certain, though silicon species incorporated into anodic alumina during anodizing in silicate electrolyte are immobile [11].

As is usual for many aluminium alloys containing alloying elements that form oxides of less negative Gibbs' free energies of formation per equivalent than that of alumina, a thin alloy layer, 1–2 nm thick, located just beneath the oxide film is enriched in the alloying elements compared with the composition of the underlying bulk phase [12, 13]. A dark band, caused by enrichment of alloying elements, has been revealed previously beneath the barrier film formed above silicide particles in borate electrolyte [10]. The alloy layer is expected to be enriched in iron, silicon and vanadium atoms, with the first predominating for the particular alloy composition as a result of its relatively high concentration in the bulk alloy and its relatively stronger tendency to enrich [13]. The enrichment of the silicide phase will occur during anodic oxidation of a few atomic layers because of the already high concentration of alloying elements in the silicide. Further, in common with certain other aluminium alloys containing alloying elements that form semiconducting oxides [14], oxygen gas is formed at high pressure within the anodic film during anodizing. An $\sim$1 nm thick dark band of alloy is also disclosed adjacent to the alloy/film interface at certain regions beneath the partially oxidized silicide beneath the porous anodic film (Fig. 5). However, the band was less clear than for the barrier film because of the greater irregularity of the alloy/film interface.

During growth of porous film material on the silicide phase, processes similar to those taking place during barrier film formation are expected, namely, enrichment of the alloy, incorporation of alloying element species into the barrier region of the film, faster migration of iron and vanadium species relative to Al^{3+} ions and production of oxygen gas. From the estimated migration rate of iron species, about 2.1 times that of Al^{3+} ions [10], the atomic ratio of Fe/Al in the oxide formed on the silicide is predicted to be $\sim$0.1 corresponding to $\sim$69% that in the bulk silicide [15]. The concentration of vanadium in the film is also expected to be reduced below the V/Al ratio, $\sim$0.025, of the bulk phase. The level of reduction is not known because of the uncertainty in the migration rate of vanadium species. Because of the probable immobility of silicon species in the anodic film, their concentration is expected to be enhanced by $\sim$67% relative to that in the bulk phase [15], namely to an Si/Al ratio of $\sim$0.10, similar to the concentration of iron species. Thus, the film material formed on the silicide is expected to contain about 20 at % of alloying element species, considering cation species only, consisting mainly of iron and silicon species. Evidently, the significantly modified alumina, with

respect to composition and probably structure, is highly soluble in the acidic pore solution.

For the modified alumina developed upon the silicide phase, the thickness of oxide formed may be either greater or less than that of the thickness of metal consumed depending especially upon the Pilling–Bedworth ratio (PBR) for the alloy. For aluminium, the PBR is $\sim$1.65. Because, in general, the ratio increases with addition of alloying element species to anodic alumina, a greater volume of oxide than of metal consumed is anticipated for the silicide phase. The volume differential is likely to produce local compressive stresses in the film near to the alloy/film interface, which reduce when the modified film material commences to dissolve. The stresses may be further augmented by local generation of oxygen bubbles within the anodic alumina formed upon the silicide phase and additionally enhanced by the irregular geometry of both the film material and the alloy/film interface. Stress generation within the anodic film may lead to film cracking, which permits access of the electrolyte to the alloy with possible oxygen evolution prior to film healing.

The development of the fine, tortuous porosity in the film material formed upon the dispersoids is probably related mainly to the influence of the modified film material on field-driven processes of dissolution of film material at the base of pores and ionic migration within the barrier layer. Although the modified film material is of relatively high solubility, the enhancement of solubility by the electric field, which is essential to formation of the porous film morphology [16], may be less than that of alumina. Hence, a higher field strength at the film/electrolyte interface may be required for a given rate of material dissolution, which can be achieved by a finer pore diameter. The presence of silicon species in the anodic film may also be important in increasing the field requirement. Notably, anodic oxidation of silicon proceeds at a field strength about four times that required for anodizing of aluminium at a similar current density [17]. The requirement for a higher field for ionic migration is compatible with the lower thickness of the barrier layer above the silicide compared with that above the aluminium matrix. On the other hand, the electric field for ionic migration is reduced by incorporation of iron species into alumina [7]. Further, the evidence from study of barrier film formation on FVS0812 suggests that thicker film regions develop above the silicide particles, which indicates a net reduction in the field for ionic migration in the contaminated film regions [10]. The reduced field for the contaminated film regions does not conflict with the lower barrier layer thickness above dispersoid material, compared with that above matrix regions, since the barrier layer thickness of porous films is influenced by field-assisted dissolution of the alumina at the pore base/electrolyte interface.

Alternatively, or in parallel with other processes, the presence of a high concentration of alloying element species in the pore solution of the porous material formed on the dispersoid phase, or adsorbed on the film surface, may inhibit field-assisted dissolution. The reduced field-assisted dissolution at the pore base leads to a slower rate of oxidation of the dispersoid compared with that of the aluminium matrix. The results of RBS and EDX indicate that the film retains significant amounts of iron and vanadium species, although at lower levels than in the bulk alloy, possibly because some of the dissolved species are adsorbed on pore walls or incorporated into gel-like material within the pores. The Si/Al ratio for the film, determined by EDX, is greater than that in the alloy by a factor of $\sim$2. The higher ratio for the film suggests that silicon species liberated by either field-assisted dissolution of material at pore bases or chemical dissolution of material formed upon silicide particles may develop a silica gel within the pores. The enhanced Si/Al ratio in the film can then be attributed to retention of silicon species while aluminium ions are lost to the solution through field-assisted dissolution of alumina.

Regions, such as those shown in Fig. 5, suggest that the rate of oxidation of the silicide, determined from the recession of the silicide/film interface, during oxidation of the silicide particle, compared with the recession of the adjacent matrix/film interface during oxidation of the matrix region, is about 80% that of the aluminium matrix [18]. Recent work has shown a parallel behaviour in the anodic oxidation of $FeAl_3$ [18]. The difference in the oxidation rates of the silicide particles and matrix regions is insufficient for undermining of particles by faster oxidation of adjacent aluminium matrix regions, prior to their complete oxidation. Thus, the anodic films contain few, if any partially oxidized dispersoid particles in the main film.

4.3. Comparison of anodizing responses of FVS0812 alloy and high purity aluminium

Apart from the morphology of the anodic film, the anodizing of FVS0812 alloy is distinguished from that of high purity aluminium by the increased steady-state voltage, namely 25 V compared with 14.6 V, and the reduced film thickness following 1800 s of film growth, namely 4.5 μm compared with 9.5 μm. Usually in anodizing of aluminium, a higher steady-state voltage is indicative of a greater thickness of barrier layer, contrary to the evidence from the FVS0812 alloy. The higher voltage may reflect the need for higher fields for ionic migration and field-assisted dissolution, as discussed previously. However, the present evidence does not support strongly the need for such large increase in the field suggested by the steady-state voltages. Alternatively, entrapment of oxygen gas within the film may increase the effective film resistance, thus requiring a higher field for film growth. The loss of efficiency due to production of oxygen, mainly above the silicide particles, then explains the reduced film thickness on the FVS0812 alloy. During anodizing of FVS0812 alloy in borate electrolyte, usual anodic film growth is effectively stopped at relatively low film thickness by extensive oxygen evolution [10]. The dissolution of porous film material formed on the

silicide particles during porous film growth results in a film that is less compact than that formed on aluminium. Consequently, the film is probably more susceptible to mechanical damage, by processes such as erosion, than films formed on more conventional aluminium alloys, as has been suggested previously [4].

5. Conclusions

1. The porous anodic film formed at 100 $A\,m^{-2}$ on FVS0812 alloy in sulphuric acid contains differently textured film material developed upon regions of silicide dispersoid and aluminium matrix. In both regions, the film porosity is more complex than that developed on high purity aluminium, with tortuous, branched and terminated pores.
2. Because of differences in the composition of film material grown at dispersoid and matrix regions, with significant influences on ionic migration in the film and field-assisted dissolution of film material at pore bases, the barrier layer thickness and porosity of the porous region are finer in the material formed upon the silicide dispersoid.
3. The growth of porous film material on the silicide dispersoid is slower than that on the aluminium matrix. However, the difference in rate is insufficient to prevent complete oxidation of the majority of the silicide particles.
4. The film material formed on the silicide particles, which contains significant amounts of alloying element species, dissolves relatively easily in the pore solution. The dissolution of the highly contaminated alumina leaves cavities in the film of dimensions similar to the original silicide particles.
5. The differing rates of oxidation of aluminium matrix and silicide regions and local differences in the properties of film material, result in a relatively rough alloy/film interface and possible stresses that may lead to film cracking.
6. Porous film growth on FVS0812 alloy proceeds at a higher voltage and with lower efficiency, than for anodizing of high purity aluminium, caused by the evolution of oxygen gas during anodizing of the alloy.

Acknowledgements

The authors are grateful to British Aerospace (Military Aircraft) for financial support of this work and to Professor G. Amsel and Dr C. Ortega for provision of time on the Van de Graaff accelerator at the University of Paris (partially funded by the Centre National de la Recherche Scientifique (GDR86)).

References

1. M. ZEDALAIS, D. RAYBOULD, D. J. SKINNER and S. K. DAS, in Processing of Structural Metals by Rapid Solidification, Florida, 1986, edited by F. H. Froes and S. J. Savage (ASM, 1987) p. 346.
2. D. J. SKINNER, R. L. BYE, D. RAYBOULD and A. M. BROWN, *Scripta Metall.* **20** (1986) 867.
3. S. C. THOMAS, V. I. BIRSS, D. STEELE and D. TESSIER, *Microsc. Res. Technique* **31** (1995) 285.
4. S. C. THOMAS and V. I. BIRSS, *J. Electrochem. Soc.* **144** (1997) 1353.
5. G. C. WOOD and A. J. BROCK, *Trans. Inst. Met. Finish.* **44** (1996) 189.
6. R. D. GUMINSKI, P. G. SHEASBY and H. J. LAMB, *ibid.* **46** (1968) 44.
7. K. SHIMIZU, G. E. THOMPSON, G. C. WOOD and K. KOBAYASHI, *J. Mater. Sci. Lett.* **10** (1991) 709.
8. L. R. DOLITTLE, *Nucl. Instr. Methods* **B15** (1986) 227.
9. J. C. CHEANG WONG, JIAN LI, C. ORTEGA, J. SIEJKA, G. VIZKELETHY and Y. LEMAITRE, *ibid.* **B64** (1992) 169.
10. J. A. SYKES, G. E. THOMPSON, D. MAYO and P. SKELDON, *J. Mater. Sci.* **32** (1997) 4909.
11. G. C. WOOD, P. SKELDON, G. E. THOMPSON and K. SHIMIZU, *J. Electrochem. Soc.* **143** (1996) 74.
12. H. HABAZAKI, K. SHIMIZU, P. SKELDON, G. E. THOMPSON, G. C. WOOD and X. ZHOU, *Corrosion Sci.* **39** (1997) 731.
13. *Idem.*, *Trans. Inst. Met. Finish.* **75** (1997) 18.
14. P. SKELDON, G. E. THOMPSON, G. C. WOOD, X. ZHOU, H. HABAZAKI and K. SHIMIZU, *Phil. Mag. A* **76** (1997) 729.
15. H. HABAZAKI, K. SHIMIZU, P. SKELDON, G. E. THOMPSON and G. C. WOOD, *Phil. Mag. B* **73** (1996) 445.
16. J. P. O'SULLIVAN and G. C. WOOD, *Proc. R. Soc. Lond A* **317** (1970) 511.
17. J. P. S. PRINGLE, *Electrochim. Acta* **25** (1980) 1423.
18. K. SHIMIZU, K. KOBAYASHI, P. SKELDON, G. E. THOMPSON and G. C. WOOD, *Corrosion Sci.*, in press.

Received 14 July 1997
and accepted 11 May 1998